BUILD SIMUL (2015) 8: 255 – 269
DOI 10.1007/s12273-015-0218-7

Experiment verified simulation study of the operating sequences on the performance of adsorption cooling system

Ka Chung Chan[1], Chi Yan Tso[1], Christopher Y.H. Chao[1] (✉), Chi Li Wu[2,3]

1. Department of Mechanical and Aerospace Engineering, The Hong Kong University of Science and Technology (HKUST), Hong Kong, China
2. Fok Ying Tung Graduate School, The Hong Kong University of Science and Technology (HKUST), Hong Kong, China
3. Guangzhou HKUST Fok Ying Tung Research Institute, Guangzhou 511485, China

Abstract

In this study, simulation was conducted to investigate the effect of heat recovery, mass recovery, pre-heating and pre-cooling processes and their combinations on the system performance of a double-bed adsorption cooling system. The model developed consists of pressure variations and detailed compressible flow with flow resistance, which other similar studies had not taken into consideration, thus a detailed simulation of mass recovery, and pre-heating and pre-cooling processes is included in this study. A double-bed adsorption cooling system with silica gel and water as adsorbent–adsorbate pair was built for verifying the simulation models. Based on the simulation results, it was found that the basic cycle provided a COP and SCP of 0.20 and 57.6 W/kg, respectively. By conducting heat recovery for 30 seconds, the COP was increased by 20% to 0.24 compared to the basic cycle. The SCP was also increased to 66.4 W/kg, a 15% increase. The major advantage through conducting the mass recovery is in the SCP, whereby it was increased by 40% to 80.8W/kg. Additionally, performing only the pre-heating and pre-cooling process can also bring some benefits to the system. Therefore, for adsorption cooling systems that cannot carry out the mass recovery and/or heat recovery cycles, performing pre-heating and pre-cooling process only is recommended. This not only can reduce the cost, but also simplify the control program of the systems. Moreover, mass recovery followed by pre-heating and pre-cooling cycle is highly preferred when the SCP is the optimization target, since the SCP was hugely increased by 41% to 81.4 W/kg.

Keywords

adsorption cooling system,
simulation,
heat and mass recovery,
operation sequence

Article History

Received: 10 November 2014
Revised: 6 January 2015
Accepted: 16 February 2015

1 Introduction

Thermal systems contribute to significant consumption of electricity in buildings. Adsorption cooling systems can be an environmentally friendly alternative to traditional vapor compression systems currently used in buildings. Adsorption cooling systems require a low-grade thermal energy source with minimal electricity required for other system components (Wang 2001; Chan et al. 2012; Tso and Chao 2012; Chua et al. 1999; Tso et al. 2012). Integrating adsorption cooling systems with solar energy or waste heat energy sources can substantially reduce the dependence on fossil fuels making these systems potential candidates for net zero energy building operation (Tso et al. 2012, 2014; Chua et al. 2004). Unlike a traditional vapor compression cooling system, the production of cooling in an adsorption cooling system is intermittent. Thus, at least two adsorbers filled with adsorbents have to be used in order to produce a quasi-continuous cooling effect (Wang et al. 2005b; Ng et al. 2006; Liu et al. 2005; Leong and Liu 2004, 2006). If the switching between the adsorption and desorption phase is not well controlled, a large amount of energy will be wasted, reducing the cooling production and efficiency (Akahira et al. 2004, 2005; Wang et al. 2007; Qu et al. 2001).

In our previous papers, a simple heat recovery was performed, in which the adsorber temperature and desorber temperature were reset by taking their average value (Tso et al. 2012, 2014). And also, mass recovery, pre-heating and pre-cooling cycles were not studied. It has also been common in many other similar studies that only heat recovery was

E-mail: meyhchao@ust.hk

List of symbols

A	heat transfer area (m^2)
c_p	specific heat capacity (J/(kg·K))
COP	coefficient of performance
D	inner diameter of pipe (m)
D_{s0}	pre-exponent constant in Eq. (4) (m^2/s)
E_a	activation energy of surface diffusion (J/mol)
f	friction factor
h_L	pressure head loss of the flow (Pa)
ΔH_s	heat of adsorption (J/kg)
K	overall mass transfer coefficient (s^{-1})
K_L	loss coefficient
l	length of pipe (m)
L	latent heat of vaporization (J/kg)
$\dot{m}$	mass flow rate (kg/s)
M	molar mass of water (g/mol)
n	number of mole
P	pressure (Pa)
P_s	saturated pressure (Pa)
R	gas constant (J/(K·mol))
R_p	radius of adsorbent particle (mm)
SCP	specific cooling power (W/kg)
T	temperature (K)
t	time (s)
U	heat transfer coefficient ($W/(m^2 \cdot K)$)
v	velocity (m/s)
V	volume (m^3)
W	mass (kg)
z	elevation (m)
ε	porosity
λ	equivalent roughness of pipe (mm)
ρ	density (kg/m^3)
ω	water uptake in the adsorbent (kg/kg)

Subscripts

ads	adsorber
chw	chilled water
cond	condenser
cu	copper
cw	water in condenser
cwa	cooling water for adsorption
cwc	cooling water for condenser
des	desorption
eva	evaporator
eq	equilibrium
hr	heat recovery
hwd	hot water for desorption
in	inlet
mr	mass recovery
out	outlet
s	adsorbent
t	adsorber tank
v	vapor
w	water

included, but neither mass recovery nor the pre-heating and pre-cooling processes of the adsorption cooling systems (Zhang and Wang 1997; Saha et al. 2003) were studied. In reality, heat recovery is a process where the thermal energy from the heated desorber is transferred to the cooled adsorber by circulating water, and this process takes time to complete. The effect was included in the simulation model. In addition, mass recovery and pre-heating and pre-cooling processes were also studied. These aspects can only be studied by taking the pressure variations of the system components into consideration. Therefore, the mathematical modeling has to be built accordingly. Chua et al. (2004) assumed that the pressure of the adsorbers was equal to that of the condenser or evaporator when they were connected to one of them. Saha et al. (2003) neglected the gas phase in the mass balance equation. Akahira et al. (2004) studied the mass recovery adsorption refrigeration cycle, but the formulation for mass recovery was not clearly stated. Wang (2001) assumed that the desorbed vapor from the high pressure adsorber is entirely re-adsorbed by the low pressure adsorber during mass recovery, without considering the mass transfer between adsorbers. Maggio et al. (2006) and Zhang (2000) set up a simulation model including the vapor diffusion inside the adsorbent bed, but not between system components. Wang et al. (2005a) utilized an incompressible flow with no flow resistance to model the vapor flow. The low pressure water vapor, however, is compressible and the pipeline might have large flow resistance on the vapor flow. Therefore, there is an urgent need to formulate the equations of water vapor flow between the system components in a more detailed simulation manner.

In this study, a detailed simulation was conducted to study the performance of the double-bed adsorption cooling system. The pressure variations of the system components and mass flow were considered in the simulation model. This simulation study aims to investigate the effect of heat recovery, mass recovery, heat recovery, pre-heating and pre-cooling processes, and their combinations, on the system performance of a double-bed adsorption cooling system. The adsorbent–adsorbate pair used was silica gel and water.

To enhance the accuracy of this simulation study, experiment results of the adsorption cooling system prototype were used to verify the simulation model. The double-bed adsorption cooling system prototype was built for a series of studies. Three sets of experiment results, different adsorption temperatures, chilled water flow rates and chilled water inlet temperature were employed for the verification process. The system description and a detailed description of those governing equations are discussed next, followed by the Results and Discussion section. The findings of the study are summarized in the Conclusion at the end of the paper.

2 System description

2.1 Basic operation phases of adsorption cooling systems

The basic cycle of operating the double-bed adsorption cooling system consists of two phases, named Phases I and II. In Phase I, adsorption takes place in Adsorber A, and desorption takes place in Adsorber B. In Phase II, desorption takes place in Adsorber A, and adsorption takes place in Adsorber B. A schematic diagram of a double-bed adsorption cooling system is shown in Fig. 1. The thinner lines represent the water pipeline for heating and cooling the adsorbers, while the thicker lines represent the low pressure pipeline for water vapor or condensed water.

The system components and the pipeline for water vapor or condensed water are evacuated before operation. Water is then introduced in to the evaporator and U-tube. The whole system is filled with low pressure water vapor. In the adsorption process, one of the adsorbers (Adsorber A) is connected to the evaporator. The water vapor is adsorbed by the silica gel adsorbent in the adsorber, maintaining a low pressure condition inside the evaporator, and thus the water can evaporate at a low temperature. Thermal energy in the chilled water is absorbed by the evaporated water. Adsorption heat is generated during the adsorption process in the adsorbent, and it has to be removed by providing the cooling water. The desorption phase takes place in a higher pressure environment. Another adsorber (Adsorber B) is heated by the hot water, and water vapor is desorbed from the adsorbent. The desorbed water vapor is transferred to the condenser by the pressure difference between the adsorber and condenser. The water vapor is cooled and condensed in the condenser, and the heat released is transferred to the cooling water. The condensed water flows back to the evaporator via the U-tube connecting the condenser and evaporator, to complete the cycle (Chua et al. 1999, 2004; Tso et al. 2012). By switching between the two phases in a double-bed adsorption cooling system, a quasi-continuous cooling effect is produced.

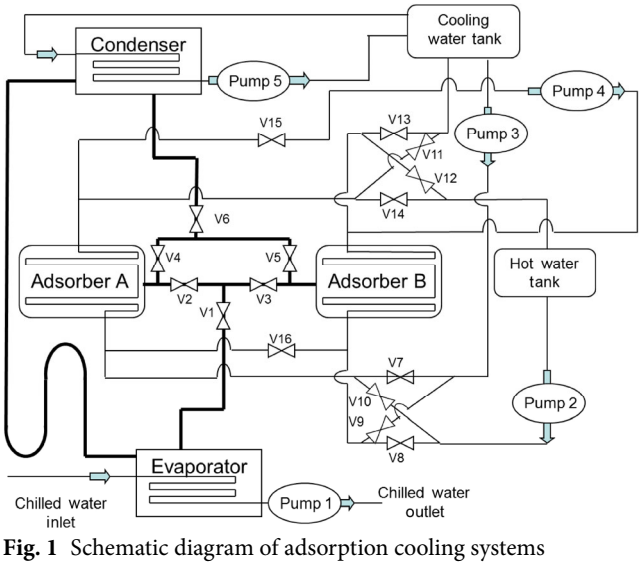

Fig. 1 Schematic diagram of adsorption cooling systems

2.2 Heat recovery process

After the desorption phase, the temperature of the corresponding adsorber is high, while the other adsorber is low after the adsorption phase. If the system were directly switched to the next operation phase, i.e. from Phase I to Phase II, most of the thermal energy in the desorber (Adsorber B) would be removed by the cooling water. As a result, a large portion of energy would be wasted. By conducting the heat recovery process between Phase I and Phase II, some thermal energy can be recovered and transferred from the heated desorber to the cooled adsorber during the phase switching. The heat transfer fluid (water) flows through the two adsorbers to transfer the heat from the heated adsorber to the cooled adsorber. By circulating the heat transfer fluid between the two adsorbers adiabatically, the energy efficiency can be enhanced significantly (Leong and Liu 2006; Wang et al. 2007; Qu et al. 2001; Pons 1997).

2.3 Mass recovery process

In the mass recovery process, the adsorbers are not connected to the evaporator and condenser. At the beginning of the mass recovery process, the heated desorber is at a higher pressure condition while the cooled adsorber is at a lower pressure condition. By connecting the two adsorbers together, the water vapor flows from the high pressure heated desorber to the low pressure cooled adsorber. Because of the pressure differences in the adsorbers, the adsorption/desorption process occurs automatically without applying either heating

or cooling. Thus, the desorbed water vapor from the heated desorber will move to the cooled adsorber. The mass recovery can further dry the heated adsorber after desorption and reduce the internal pressure. The dryer adsorber can adsorb more water vapor in the next adsorption phase. The process leads the adsorption cooling systems to provide a better performance (Wang 2001; Ng et al. 2006; Leong and Liu 2006; Akahira et al. 2004, 2005; Wang et al. 2007; Qu et al. 2001).

2.4 Pre-heating and pre-cooling process

The pre-heating and/or pre-cooling process is in fact a pre-conditioning process. After the adsorption phase, the internal pressure of the adsorber is low. If it were immediately connected to the condenser, water in the condenser would evaporate and flow back to the adsorber. This would increase the water uptake of the adsorbent in the adsorber and lower the system performance. A similar drawback would also appear on the desorption side. Hence, the pressure of the desorber has to be increased and that of the adsorber has to be decreased before connection to the condenser and evaporator. The cooling water is connected to the desorber (the adsorber in the next phase), and the hot water is connected to the adsorber (the desorber in the next phase). When the pressures of the desorber and adsorber are nearly equal to the pressures of the condenser and evaporator respectively, the corresponding system components are connected.

3 Mathematical model

3.1 Assumptions

The following assumptions were made in the simulation:

1) The temperature, pressure and the amount of water vapor adsorbed are uniform throughout the adsorbent beds.
2) There is no external heat loss to the surroundings as all the system components are assumed to be well-insulated.
3) The condensate can flow into the evaporator easily, so the amount of water inside the condenser is unchanged.
4) The water vapor flows among the evaporator, adsorbers and condenser are only driven by the pressure difference between two system components.
5) The water vapor condenses immediately in the condenser without superheating.
6) The water evaporates instantaneously in the evaporator without supercooling.
7) The adsorbed phase is considered as a liquid and the adsorbate gas is assumed to be an ideal gas.
8) The thermal resistance between the metal tube and the adsorbent bed is neglected.
9) Flow resistance arising from the water flowing in the pipeline is neglected.
10) The properties of the fluid, the metal tube and adsorbate vapor are constant.

According to these assumptions, the dynamic behavior of heat and mass transfer inside the different system components of the adsorption cooling system can be written as shown below.

3.2 Equilibrium water uptake

The adsorption equilibrium for silica gel/water is expressed by the following correlation based on the study conducted by Sakoda and Suzuki (1984):

$$\omega_{eq} = 0.346\left[P_w / P_s(T_s)\right]^{1/1.6} \tag{1}$$

where ω_{eq} is the equilibrium amount of water uptake in the adsorbent, P_w is the water vapor pressure inside the adsorber, T_s is the adsorbent temperature, and $P_s(T_s)$ is the corresponding saturated vapor pressure under the adsorbent temperature. The saturated vapor pressure is calculated by the Antoine equation (Dean and Lange 1999):

$$\log_{10} P_s = 8.07131 - \frac{1730.63}{T - 39.574} \tag{2}$$

In Eq. (2), the unit of vapor pressure is mmHg, while the unit in other equations of this study is Pa.

3.3 Adsorption rate

The adsorption process in an adsorbent bed is considered to be controlled by surface diffusion inside the adsorbent particles. Using a linear driving force equation (Sakoda and Suzuki 1984), the adsorption rate is proportional to the difference between the concentrations of equilibrium and present state. Therefore, it is expressed as

$$\frac{d\omega}{dt} = K\left(\omega_{eq} - \omega\right) \tag{3}$$

where K is the overall mass transfer coefficient, and is calculated by

$$K = \frac{15 D_{s0}}{R_p^2} \exp\left(\frac{-E_a}{RT}\right) \tag{4}$$

where D_{s0} is the pre-exponent constant, E_a is the activation energy of surface diffusion, R is the gas constant, and R_p is the radius of the adsorbent particle.

3.4 Energy and mass balance for the adsorber

To simplify the simulation process, one of the two adsorbent beds is treated as the adsorber during the adsorption phase, and is treated as the desorber during the desorption phase. In the simulation, the Adsorbers A and B alternate their roles of adsorption and desorption. In other words, Adsorber A is treated as the adsorber in each odd iteration while it is treated as the desorber in each even iteration. The energy balance for the adsorber is described by

$$\begin{aligned}&\frac{\mathrm{d}}{\mathrm{d}t}\left[\left(W_{\mathrm{s}}c_{\mathrm{p,s}}+W_{\mathrm{s}}c_{\mathrm{p,w}}\omega_{\mathrm{ads}}+W_{\mathrm{cu,ads}}c_{\mathrm{p,cu}}\right)T_{\mathrm{ads}}\right]\\&=\Delta H_{\mathrm{s}}W_{\mathrm{s}}\frac{\mathrm{d}\omega_{\mathrm{ads}}}{\mathrm{d}t}+\dot{m}_{\mathrm{v,ads}}c_{\mathrm{p,v}}\left(T_{\mathrm{eva}}-T_{\mathrm{ads}}\right)\\&\quad+\dot{m}_{\mathrm{cwa}}c_{\mathrm{p,w}}\left(T_{\mathrm{cwa,in}}-T_{\mathrm{cwa,out}}\right)\end{aligned}\tag{5}$$

where W_{s} is the mass of silica gel in the adsorber, c_{p} is the specific heat capacity of different materials, ω_{ads} is the water uptake in the adsorber, $\dot{m}_{\mathrm{v,ads}}$ is the mass transfer rate of water vapor from the evaporator to the adsorber, the subscript *cu* represents the copper tube for heat transfer, and *cwa* represents the cooling water for adsorption. The left hand side of Eq. (5) represents the rate of sensible heat change of the adsorber including the silica gel, adsorbed water and copper tube. The first term on the right hand side of Eq. (5) represents the adsorption heat released or gained. Due to the fact that the adsorption process is an exothermic reaction, the first term is positive when adsorption occurs and the rate of adsorption is also positive accordingly. The second term represents the energy change because of the water vapor flowing from the evaporator. The last term indicates the amount of heat transferred to the cooling water during adsorption. The outlet temperature of the cooling water is expressed as

$$T_{\mathrm{cwa,out}}=T_{\mathrm{ads}}+\left(T_{\mathrm{cwa,in}}-T_{\mathrm{ads}}\right)\exp\left(\frac{-U_{\mathrm{ads}}A_{\mathrm{ads}}}{\dot{m}_{\mathrm{cwa}}c_{\mathrm{p,w}}}\right)\tag{6}$$

where U_{ads} is the heat transfer coefficient of the adsorber, and A_{ads} is the heat transfer area of the adsorber. In order to simulate the mass transfer between the evaporator, two adsorbent beds and the condenser, the water vapor flow rate is assumed to be a pressure driven pipe flow with negligible effect from diffusion. Thus, the flow rate (v) is calculated from

$$P_1+\frac{1}{2}\rho_1 v_1^2+z_1=P_2+\frac{1}{2}\rho_2 v_2^2+z_2+h_{\mathrm{L}}\tag{7}$$

where the subscript 1 represents the place with higher pressure, h_{L} is the head loss of the flow. Equation (7) is then simplified to

$$\Delta P=\frac{1}{2}\rho v^2+h_{\mathrm{L}}\tag{8}$$

by ignoring the evaluation change and the initial flow rate. The head loss consists of major and minor losses. The major loss is due to the stress force between the flow and the pipe wall, and is given by (Munson et al. 2006)

$$h_{\mathrm{L,major}}=f\frac{1}{2}\frac{\rho l}{D}v^2\tag{9}$$

where l and D are the length and inner diameter of the pipe, respectively. f is the friction factor, depending on the Reynolds number and the ratio of equivalent roughness (λ) to pipe diameter. As the kinematic viscosity of water vapor is very small, the flow is assumed to be a turbulent flow, and this is verified later in this section. The Colebrook formula is then used to find the friction factor, which is (Munson et al. 2006)

$$\frac{1}{\sqrt{f}}=-2\log\left(\frac{\lambda/D}{3.7}+\frac{2.51}{Re\sqrt{f}}\right)\tag{10}$$

Another head loss is the minor loss, caused by valves, bends, contraction and expansion of the pipe, etc. The minor loss is expressed as

$$h_{\mathrm{L,minor}}=K_{\mathrm{L}}\frac{1}{2}\rho v^2\tag{11}$$

where K_{L} is the loss coefficient, calculated at about 5 according to a lab-scaled adsorption cooling system prototype. Equations (9) and (11) are substituted into Eq. (8) to find the flow rate. It was found that the Reynolds number is about 4000 when the pressure difference is 300 Pa at 5℃. If the pressure difference is larger or the vapor temperature is higher, the Reynolds number will increase. This proves that the water vapor flow is turbulent. The flow rate is then multiplied with the density and cross section area of the pipe to find the water vapor mass flow rate, $\dot{m}_{\mathrm{v}}$.

The water vapor mass balance inside the adsorber is given by

$$\frac{\partial\left(V_{\mathrm{s}}\varepsilon+V_{\mathrm{t}}\right)\rho_{\mathrm{v,ads}}}{\partial t}=\dot{m}_{\mathrm{v,ads}}-V_{\mathrm{s}}\rho_{\mathrm{s}}\frac{\partial\omega_{\mathrm{ads}}}{\partial t}\tag{12}$$

where V_{s} and V_{t} are the volume of the adsorbent and the adsorber tank respectively, ε is the porosity of the adsorbent. By using the ideal gas law, the water vapor density is found:

$$PV=nRT\Rightarrow PV=\frac{W_{\mathrm{v}}}{M}RT\Rightarrow\rho_{\mathrm{v}}=\frac{PM}{RT}\tag{13}$$

where M is the molar mass of water. Then, Eq. (12) becomes

$$\frac{\partial P_{\mathrm{ads}}}{\partial t}=\frac{RT_{\mathrm{ads}}}{M\left(V_{\mathrm{s}}\varepsilon+V_{\mathrm{t}}\right)}\left(\dot{m}_{\mathrm{v,ads}}-V_{\mathrm{s}}\rho_{\mathrm{s}}\frac{\partial\omega_{\mathrm{ads}}}{\partial t}\right)\tag{14}$$

where P_{ads} is the pressure in the adsorber.

3.5 Energy and mass balance for the desorber

Similar to the adsorber, the adsorbent bed is treated as the desorber when the desorption phase occurs. The energy balance for the desorber is described by

$$\frac{\mathrm{d}}{\mathrm{d}t}\left[\left(W_{\mathrm{s}}c_{\mathrm{p,s}}+W_{\mathrm{s}}c_{\mathrm{p,w}}\omega_{\mathrm{des}}+W_{\mathrm{cu,des}}c_{\mathrm{p,cu}}\right)T_{\mathrm{des}}\right] = \Delta H_{\mathrm{s}}W_{\mathrm{s}}\frac{\mathrm{d}\omega_{\mathrm{des}}}{\mathrm{d}t}+\dot{m}_{\mathrm{hwd}}c_{\mathrm{p,w}}\left(T_{\mathrm{hwd,in}}-T_{\mathrm{hwd,out}}\right) \quad (15)$$

where ω_{des} is the water uptake in the desorber and the subscript *hwd* represents the hot water for desorption. The adsorption heat term on the right hand side is negative when desorption occurs and the rate of adsorption is also negative accordingly. This represents that energy is supplied to desorb water vapor out from the silica gel. The second term represents the amount of heat provided by the hot water supply. The outlet temperature of the hot water is expressed as

$$T_{\mathrm{hwd,out}} = T_{\mathrm{des}}+\left(T_{\mathrm{hwd,in}}-T_{\mathrm{des}}\right)\exp\left(\frac{-U_{\mathrm{des}}A_{\mathrm{des}}}{\dot{m}_{\mathrm{hwd}}c_{\mathrm{p,w}}}\right) \quad (16)$$

where U_{des} is the heat transfer coefficient of the desorber, and A_{des} is the heat transfer area of the desorber. The water vapor mass balance inside the desorber is given by

$$\frac{\partial\left(V_{\mathrm{s}}\varepsilon+V_{\mathrm{t}}\right)\rho_{\mathrm{v,des}}}{\partial t} = -\dot{m}_{\mathrm{v,des}}-V_{\mathrm{s}}\rho_{\mathrm{s}}\frac{\partial\omega_{\mathrm{des}}}{\partial t} \quad (17)$$

It is then transformed to

$$\frac{\partial P_{\mathrm{des}}}{\partial t} = -\frac{RT_{\mathrm{des}}}{M\left(V_{\mathrm{s}}\varepsilon+V_{\mathrm{t}}\right)}\left(\dot{m}_{\mathrm{v,des}}+V_{\mathrm{s}}\rho_{\mathrm{s}}\frac{\partial\omega_{\mathrm{des}}}{\partial t}\right) \quad (18)$$

3.6 Energy balance for the condenser

The condenser energy balance equation is written as

$$\frac{\mathrm{d}T_{\mathrm{cond}}}{\mathrm{d}t}\left(W_{\mathrm{cu,cond}}c_{\mathrm{p,cu}}+W_{\mathrm{cw}}c_{\mathrm{p,w}}\right) = \dot{m}_{\mathrm{v,des}}c_{\mathrm{p,v}}\left(T_{\mathrm{des}}-T_{\mathrm{cond}}\right)+L_{\mathrm{w}}\dot{m}_{\mathrm{v,des}}+\dot{m}_{\mathrm{cwc}}c_{\mathrm{p,w}}\left(T_{\mathrm{cwc,in}}-T_{\mathrm{cwc,out}}\right) \quad (19)$$

where W_{cw} is the weight of water inside the condenser, L_{w} is the latent heat of the vaporization of the water and the subscript *cwc* represents the cooling water for the condenser. The left hand side represents the sensible heat change of the copper tube and water in the condenser. The first term on the right hand side represents the sensible heat change of the water vapor from the temperature of the desorber to that of the condenser. The second term is the latent heat change of the water vapor to condensed water, and the last term is the amount of heat transferred to the cooling water. The outlet temperature of the cooling water for the condenser is given as

$$T_{\mathrm{cwc,out}} = T_{\mathrm{cond}}+\left(T_{\mathrm{cwc,in}}-T_{\mathrm{cond}}\right)\exp\left(\frac{-U_{\mathrm{cond}}A_{\mathrm{cond}}}{\dot{m}_{\mathrm{cwc}}c_{\mathrm{p,w}}}\right) \quad (20)$$

There is no mass balance equation for the condenser because the amount of water inside the condenser is assumed to be constant.

3.7 Energy and mass balance for the evaporator

The energy balance in the evaporator is expressed as

$$\frac{\mathrm{d}T_{\mathrm{eva}}}{\mathrm{d}t}\left(W_{\mathrm{eva}}c_{\mathrm{p,w}}+W_{\mathrm{cu,eva}}c_{\mathrm{p,cu}}\right) = -L_{\mathrm{w}}\dot{m}_{\mathrm{v,ads}}+c_{\mathrm{p,w}}\left(T_{\mathrm{con}}-T_{\mathrm{eva}}\right)\dot{m}_{\mathrm{v,des}} +\dot{m}_{\mathrm{chw}}c_{\mathrm{p,w}}\left(T_{\mathrm{chw,in}}-T_{\mathrm{chw,out}}\right) \quad (21)$$

where W_{eva} is the weight of water inside the evaporator. The first term on the right hand side represents the latent heat change of the water to water vapor, and the water vapor is transferred from the evaporator to the adsorber. The second term represents the sensible heat change of the water flowing back from the condenser to the evaporator. The last term represents the cooling load transferred to the chilled water. The outlet temperature of the chilled water is written as

$$T_{\mathrm{chw,out}} = T_{\mathrm{eva}}+\left(T_{\mathrm{chw,in}}-T_{\mathrm{eva}}\right)\exp\left(\frac{-U_{\mathrm{eva}}A_{\mathrm{eva}}}{\dot{m}_{\mathrm{chw}}c_{\mathrm{p,w}}}\right) \quad (22)$$

The mass balance of the water in the evaporator is written as

$$\frac{\mathrm{d}W_{\mathrm{eva}}}{\mathrm{d}t} = -\dot{m}_{\mathrm{v,ads}}+\dot{m}_{\mathrm{v,des}} \quad (23)$$

3.8 Measurement of system performance

The specific cooling power (SCP) of the system is expressed by

$$\mathrm{SCP} = \frac{\dot{m}_{\mathrm{chw}}c_{\mathrm{p,w}}\int_0^{t_{\mathrm{cycle}}}\left(T_{\mathrm{chw,in}}-T_{\mathrm{chw,out}}\right)\mathrm{d}t}{W_{\mathrm{s}}t_{\mathrm{cycle}}} \quad (24)$$

where t_{cycle} is the total cycle duration.

The COP value is defined by the following equation:

$$\mathrm{COP} = \frac{\dot{m}_{\mathrm{chw}}c_{\mathrm{p,w}}\int_0^{t_{\mathrm{cycle}}}\left(T_{\mathrm{chw,in}}-T_{\mathrm{chw,out}}\right)\mathrm{d}t}{\dot{m}_{\mathrm{hwd}}c_{\mathrm{p,w}}\int_0^{t_{\mathrm{cycle}}}\left(T_{\mathrm{hwd,in}}-T_{\mathrm{hwd,out}}\right)\mathrm{d}t} \quad (25)$$

It is assumed that the adsorption cooling system is powered by low-grade thermal energy sources, like solar energy or waste heat from industrial processes. Thus, the thermal energy required by the adsorption cooling system

can be considered to be free and the COP is much less important than the SCP. The SCP is treated as the main optimization target in this study.

3.9 Equations modified for heat recovery

In heat recovery, the water for heat transfer is circulated between two adsorbers under the mass flow rate of $\dot{m}_{hr}$. Thus, Eqs. (6) and (16) are modified to

$$T_{cwa,out} = T_{ads} + (T_{hwd,out} - T_{ads})\exp\left(\frac{-U_{ads}A_{ads}}{\dot{m}_{hr}c_{p,w}}\right) \quad (26)$$

and

$$T_{hwd,out} = T_{des} + (T_{cwa,out} - T_{des})\exp\left(\frac{-U_{des}A_{des}}{\dot{m}_{hr}c_{p,w}}\right) \quad (27)$$

respectively. There is also no water vapor mass transfer between system components during heat recovery ($\dot{m}_{v,ads} = 0$ and $\dot{m}_{v,des} = 0$), so Eqs. (5) and (15) are modified to

$$\frac{d}{dt}\left[\left(W_s c_{p,s} + W_s c_{p,w}\omega_{ads} + W_{cu,ads}c_{p,cu}\right)T_{ads}\right] = \Delta H_s W_s \frac{d\omega_{ads}}{dt} + \dot{m}_{hr}c_{p,w}\left(T_{cwa,in} - T_{cwa,out}\right) \quad (28)$$

and

$$\frac{d}{dt}\left[\left(W_s c_{p,s} + W_s c_{p,w}\omega_{des} + W_{cu,des}c_{p,cu}\right)T_{des}\right] = \Delta H_s W_s \frac{d\omega_{des}}{dt} + \dot{m}_{hr}c_{p,w}\left(T_{hwd,in} - T_{hwd,out}\right) \quad (29)$$

respectively.

3.10 Equations modified for mass recovery

In mass recovery, the adsorber and desorber are connected to each other. Water vapor will flow from the high-pressured desorber to the low-pressured adsorber with a mass flow rate of $\dot{m}_{mr}$. Thus, Eqs. (14) and (18) are modified to

$$\frac{\partial P_{ads}}{\partial t} = \frac{RT_{ads}}{M\left(V_s\varepsilon + V_t\right)}\left(\dot{m}_{mr} - V_s\rho_s\frac{\partial\omega_{ads}}{\partial t}\right) \quad (30)$$

and

$$\frac{\partial P_{des}}{\partial t} = -\frac{RT_{des}}{M\left(V_s\varepsilon + V_t\right)}\left(\dot{m}_{mr} + V_s\rho_s\frac{\partial\omega_{des}}{\partial t}\right) \quad (31)$$

respectively. There is no water circulating inside the adsorbers and desorbers ($\dot{m}_{cwa} = 0$ and $\dot{m}_{hwd} = 0$), so Eqs. (5) and (15) are modified to

$$\frac{d}{dt}\left[\left(W_s c_{p,s} + W_s c_{p,w}\omega_{ads} + W_{cu,ads}c_{p,cu}\right)T_{ads}\right] = \Delta H_s W_s \frac{d\omega_{ads}}{dt} + \dot{m}_{mr}c_{p,v}\left(T_{eva} - T_{ads}\right) \quad (32)$$

and

$$\frac{d}{dt}\left[\left(W_s c_{p,s} + W_s c_{p,w}\omega_{des} + W_{cu,des}c_{p,cu}\right)T_{des}\right] = \Delta H_s W_s \frac{d\omega_{des}}{dt} \quad (33)$$

respectively. In addition, the equation modifications for both heat and mass recovery are the combination of heat recovery and mass recovery.

3.11 Equations modified for pre-heating and pre-cooling process

Similar to the modifications made for heat recovery, there is also no water vapor mass transfer between system components during the pre-heating and pre-cooling process. Cooling water and hot water are circulated to the desorber and adsorber, respectively.

3.12 Simulation procedures and conditions

The system of differential equations listed above is solved simultaneously by the finite difference method. The implicit method is applied to treat the time derivative to improve the stability of the simulation. In each time step, an initial guess based on the previous time step is used and the value of each variable is accepted when the difference between the current estimated value and the previous one is smaller than 10^{-6}. A small time step of 4×10^{-3} seconds is employed and it is stable for all simulations. The simulation ends when the differences in SCP and COP of the current cycle and the previous cycle are smaller than 1%. The values of parameters used in the simulation are based on a lab-scale prototype previously built by us. The simulation parameters were verified by comparing the simulation results with the experiment and the comparison is presented in a later section of this paper. The standard chilled water inlet temperature is set at 14℃ since this is a typical chilled water return temperature in buildings. The cooling source temperature is set at 27℃ with the consideration of utilizing a cooling tower. The hot water source is set at 85℃ as this temperature can be achieved by most of the evacuated tube solar collectors. The varied operating sequence for the adsorption cooling system is shown in Table 1. The durations of heat recovery, mass recovery, and heat and mass recovery are studied to predict their effect on the system performance.

Table 1 Operating sequences of the system (I: Phase I; II: Phase II; HR: heat recovery; MR: mass recovery; Pre-HC: pre-heating and pre-cooling; HMR: heat and mass recovery)

	Operating sequences
Basic cycle	I → II → I …
Heat recovery cycle	I → HR → II → HR→ I …
Mass recovery cycle	I → MR → II → MR→ I …
Pre-heating and pre-cooling cycle	I → Pre-HC → II → Pre-HC → I …
Heat and mass recovery cycle	I → HMR → II → HMR→ I …
HR followed by Pre-HC cycle	I → HR → Pre-HC → II → HR→ Pre-HC → I …
MR followed by Pre-HC cycle	I → MR → Pre-HC → II → MR→ Pre-HC → I …
HMR followed by Pre-HC cycle	I → HMR → Pre-HC → II → HMR→ Pre-HC → I …

4 Results and discussion

4.1 System parameters verification

Before conducting a detailed simulation study about different operation sequences, the system parameters were verified by the experiment results of the double-bed adsorption cooling system prototype. Two adsorbers were designed and built based on the consideration of the heat and mass transfer abilities of the adsorbers, which can affect the system performance. Each adsorber consisted of 14 cylindrical shell units covered with a stainless steel metal screen mesh with a pore size of about 74 μm. Figure 2 shows a photograph of a cylindrical shell unit. The adsorbents were packed between the circular fins. Each adsorber was filled with 9 kg of silica gel adsorbent. 14 cylindrical shell units were put together into a large cylindrical vacuum chamber (adsorber), connected in series by copper piping as shown in Fig. 3. A photograph of the whole adsorption cooling system prototype is also shown in Fig. 4.

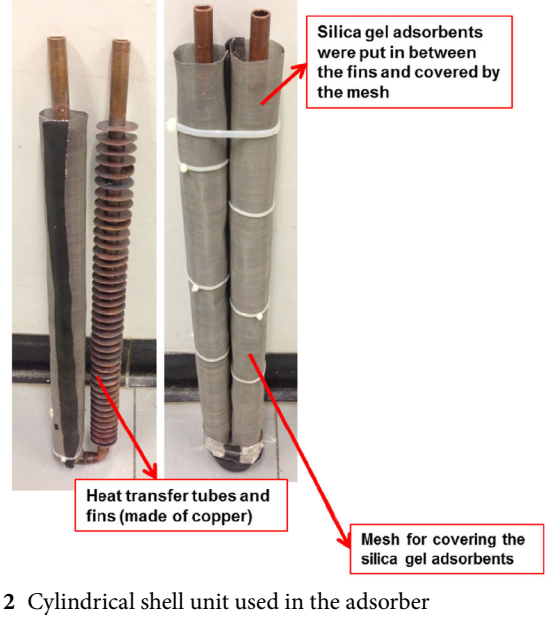

Fig. 2 Cylindrical shell unit used in the adsorber

Some values of parameters were found by a direct measurement from a lab-scale prototype, including inlet water temperatures, water flow rates, adsorbent size, masses and heat transfer areas of system components. The overall heat transfer coefficients, however, cannot be directly measured. Thus, the experimental system performance

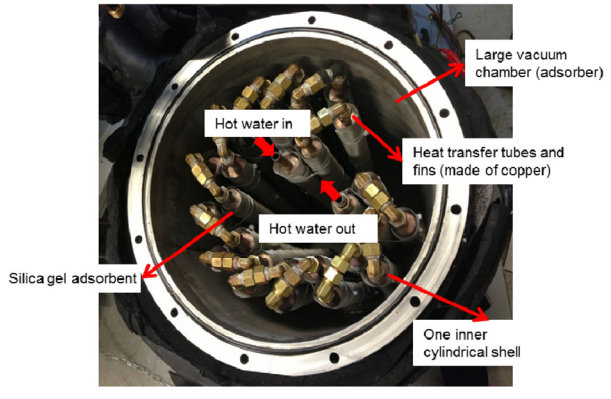

Fig. 3 14 cylindrical shells in a large vacuum chamber (adsorber)

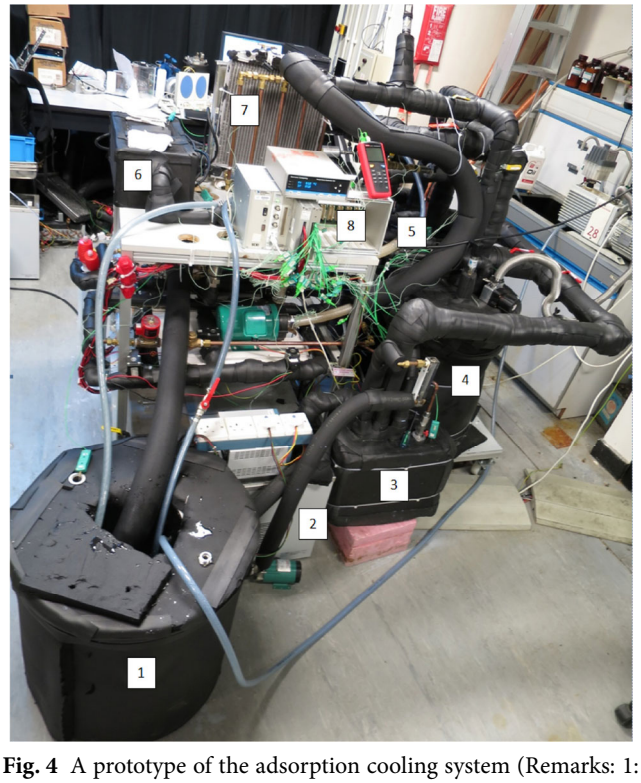

Fig. 4 A prototype of the adsorption cooling system (Remarks: 1: cooling water tank; 2: isothermal water circulator; 3: chilled water tank (evaporator); 4: Adsorber A; 5: Adsorber B; 6: hot water tank; 7: condenser; 8: control system)

under different adsorption temperatures, chilled water flow rates and chilled water inlet temperatures were used to estimate the overall heat transfer coefficients. The overall heat transfer coefficients of the adsorber, desorber, condenser and evaporator were adjusted until the simulation results were in a good agreement with the experiment. Figure 5 shows a comparison between the experiment and simulation results with different adsorption temperatures. The average absolute error of the specific cooling power (SCP) between the experiment and simulation results is 5.8%, and that of the COP is 4.1%. Moreover, the error of the SCP and COP are 0.2% and 0.1% respectively when the adsorption temperature is 27℃, which is the standard value of this simulation study. It can also be seen that the performance of the lab-scale prototype presented in the current study is not as good as that presented in other simulation studies. For example, Chua et al. (1999) estimated that the SCP and COP predicted from their simulation were 313 W/kg and 0.42, respectively, while the SCP and COP predicted from this study were 68 W/kg and 0.30. This is because the simulations were based on different values for the parameters. One of the major differences is the mass of adsorbent used. In the paper of (Chua et al. 1999), 47 kg of silica gel was used, while only 9 kg was used in this study. Besides, the values of parameters were adjusted according to the real experiment result in this study. The effect of heat loss to the surrounding was also included. This effect is significant when the mass of adsorbent used is comparatively small.

The simulation result is then compared to the experiment with different chilled water flow rates as shown in Fig. 6. It can be seen that the simulation result is in good agreement with the experiment, except for the highest flow rate, 7.6 kg/min. The average errors of the SCP and COP are 4.2% and 2.8% respectively, while the error of the SCP for the highest flow rate is 11.2%. Theoretically, the overall heat transfer is better for a higher flow rate, leading to a better

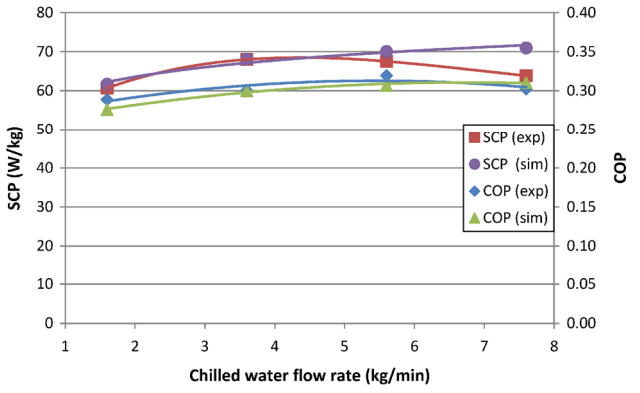

Fig. 6 Comparison between experiment and simulation results with different chilled water flow rates (exp: experiment; sim: simulation)

system performance. The same trend can also be observed in the simulation result, but the experiment result of the SCP decreases at a higher flow rate. This might be due to a larger heat loss to the surroundings under a higher flow rate in the real experiment. A comparison with different chilled water inlet temperatures is also shown in Fig. 7. Similar to the effect of changing the chilled water flow rate, there is a larger error with a lower chilled water inlet temperature. The errors reduce with an increase of inlet temperature, and the error of the SCP with a standard chilled water inlet temperature, 14℃, is 1.6% only. Overall, it can be concluded that the simulation can well predict the real performance of the adsorption cooling systems. Based on the verification, the system parameters adopted in the simulation are listed in Table 2. The values of overall heat transfer coefficient of adsorber and desorber are lower than those presented by other similar studies (Chua et al. 1999; Saha et al. 2003). The reason is that heat is lost to the surrounding during transferring to or from the adsorbent, and it is impossible to distinguish the individual contribution of heat loss from

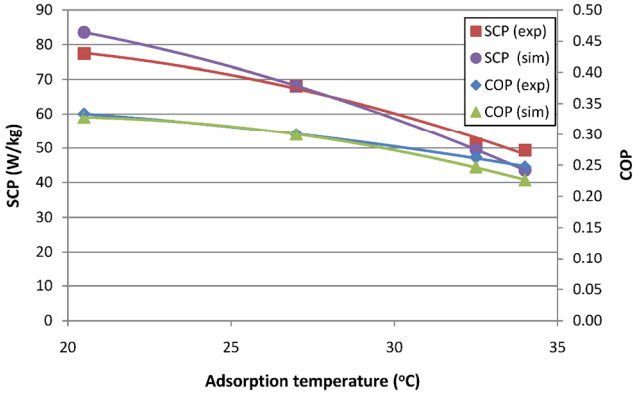

Fig. 5 Comparison between experiment and simulation results with different adsorption temperatures (exp: experiment; sim: simulation)

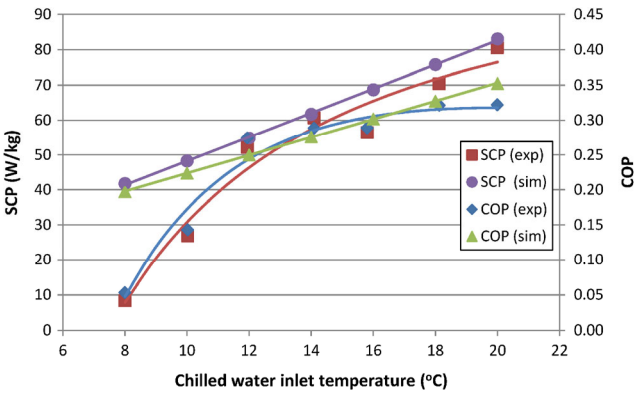

Fig. 7 Comparison between experiment and simulation results with different chilled water inlet temperatures (exp: experiment; sim: simulation)

Table 2 The values of parameters adopted in the simulation

Symbol	Value	Unit	Symbol	Value	Unit
A_{ads}	2.11	m^2	t_{mass}	10	s
A_{des}	2.11	m^2	$T_{chw,in}$	14	℃
A_{cond}	5.76	m^2	$T_{cwa,in}$	27	℃
A_{eva}	0.34	m^2	$T_{cwc,in}$	27	℃
$c_{p,cu}$	386	J/(kg·K)	$T_{hwd,in}$	85	℃
$c_{p,s}$	924	J/(kg·K)	U_{ads}	189.60	W/(m^2·K)
ΔH_s	2.80×10^6	J/kg	U_{des}	203.99	W/(m^2·K)
D_{s0}	2.54×10^{-4}	m^2/s	U_{cond}	486.87	W/(m^2·K)
E_a	4.2×10^4	J/mol	U_{eva}	302.58	W/(m^2·K)
$\dot{m}_{chw}$	1.6	kg/min	V_t	0.5	m^3
$\dot{m}_{cwa}$	8	kg/min	$W_{cu,ads/des}$	65	kg
$\dot{m}_{cwc}$	20	kg/min	W_s	9	kg
$\dot{m}_{hwd}$	7	kg/min	$W_{cu,eva}$	16.1	kg
M	18.02	g/mol	$W_{cu,cond}$	19.87	kg
R_p	0.56	mm	W_{cw}	1	kg
t_{phase}	15	min	ρ_s	2000	kg/m^3
t_{heat}	50	s	ε	0.3	—

overall heat transfer. Under a larger heat loss, less energy can be transferred to the adsorbent. This effect is modelled by analogy with a lower value of overall heat transfer coefficient.

4.2 Basic cycle performance

The basic cycle was simulated to obtain the reference performance of the system, to serve as the baseline for different operation sequences. As presented in Table 1, the basic cycle's COP and SCP of the adsorption cooling system were calculated to be 0.20 and 57.6 W/kg, respectively. A temperature profile of the system components and the water inlet and outlet in different locations of the last two cycles is shown in Fig. 8, and a pressure profile is shown in Fig. 9. It is shown that at the beginning of Phases I and II,

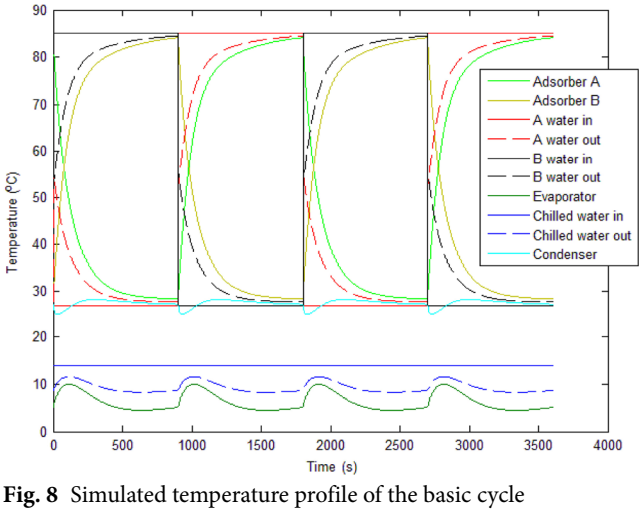

Fig. 8 Simulated temperature profile of the basic cycle

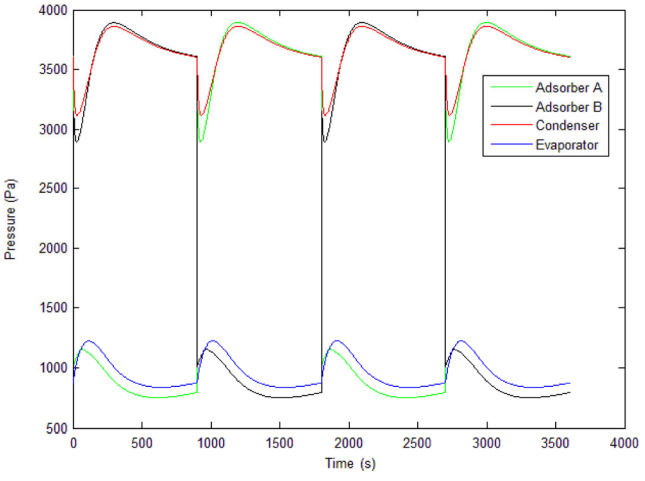

Fig. 9 Simulated pressure profile of the basic cycle

the chilled water outlet temperature increases because of the increase of the evaporator temperature. This indicates that water vapor from the adsorber is transferred to and condensed in the evaporator. This phenomenon can also be seen from the pressure profile shown in Fig. 9. The pressure in the evaporator increases sharply, proving the high pressure water vapor flows from the adsorber to the evaporator. A similar effect can also be observed in the condenser. This indicates the need for mass recovery and/or pre-heating and pre-cooling cycles in adsorption cooling systems.

4.3 Effect of heat recovery cycle

The heat recovery is to transfer the thermal energy of the heated desorber to the cooled adsorber, and this process is presented in a detailed temperature profile in Fig. 10. The temperatures of Adsorbers A and B converge indicating the

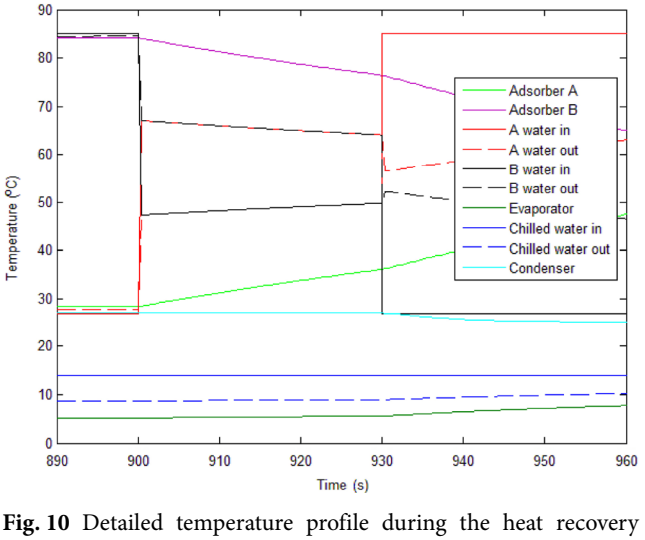

Fig. 10 Detailed temperature profile during the heat recovery process

thermal energy is transferred. The effect of heat recovery on the performance of the adsorption cooling system is represented in Fig. 11. It can be seen in Fig. 11 that a longer heat recovery phase time can give a higher COP. The COP reached 0.29, a 45% improvement, when the duration of heat recovery was 90 seconds. This trend indicates that the COP can be further improved for a longer heat recovery phase time. This is because more heat can be recovered from the heated desorber to the cooled adsorber, reducing the thermal energy required to heat the adsorber for the next desorption phase. On the other hand, a maximum SCP of 66.4 W/kg, a 15% improvement, is obtained with a heat recovery duration of 30 seconds. The SCP decreases beyond this point since there is no cooling effect produced during the heat recovery phase. In other words, a longer heat recovery phase diminishes the cooling performance of the adsorption cooling systems. With regard to this, performing the heat recovery cycle can significantly increase the COP of the adsorption cooling systems, and also can slightly enhance its SCP.

4.4 Effect of mass recovery cycle

Figure 12 shows the effect of the duration of the mass recovery process on the system performance. A peak for the SCP was found at 100 seconds, at which its value was calculated as 80.8 W/kg, a 40% enhancement compared to that of the basic cycle. The increase in the SCP is the result of the water vapor transfer from the high-pressured desorber to the low-pressured adsorber. The desorber can quickly decrease its pressure for the next adsorption phase, while the adsorber can quickly increase its pressure for the next desorption phase. The desorber can also be further dried through this process. For an extended mass recovery phase time, the water vapor transfer between the two adsorbers slows down. Similar to the effect of an extended heat recovery phase time, the SCP decreases beyond this point. It is also interesting to note that the COP is increased by 14% to 0.23. The increase in the COP may be because of the large increase in the SCP. The COP was calculated by Eq. (25) where the system's total cooling power is in the numerator. With the same system, the mass of copper utilized in the system's components is the same and this mass reduces the COP from the ideal value. A larger total cooling power can separate the loading caused by the mass of system components. The increase in system's cooling power can, thus, indirectly increase the COP.

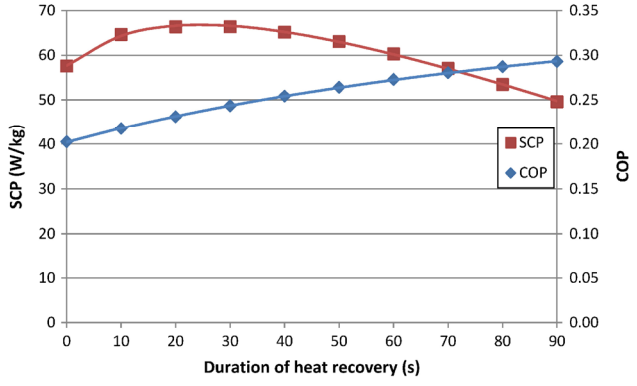

Fig. 11 Effect of the duration of heat recovery on system performance

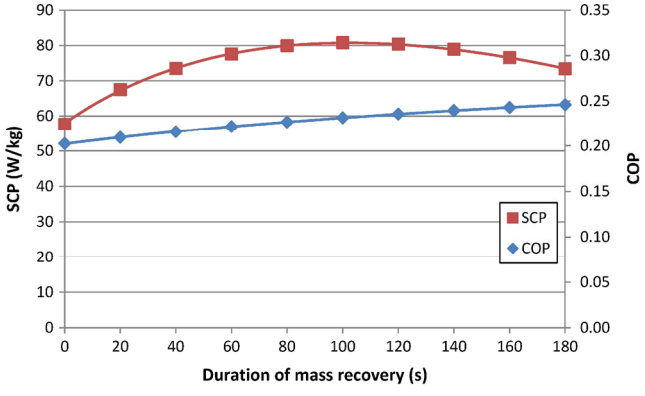

Fig. 12 Effect of the duration of mass recovery on system performance

4.5 Effect of pre-heating and pre-cooling cycle

The effect of the duration of pre-heating and pre-cooling in pre-heating and pre-cooling cycle on system performance is shown in Fig. 13. The maximum SCP was found at 30 seconds, improved by 17% to 67.7 W/kg. The reason for the peak of the SCP can be found in a detailed pressure profile during the pre-heating and pre-cooling process as shown in Fig. 14. In Fig. 14, the pre-heating and pre-cooling process is carried out until the pressure of Adsorber B is lower than that of the evaporator. The pressure of Adsorber B decreases from above 3,500 Pa and is lower than that of the evaporator when the pre-heating and pre-cooling process is stopped.

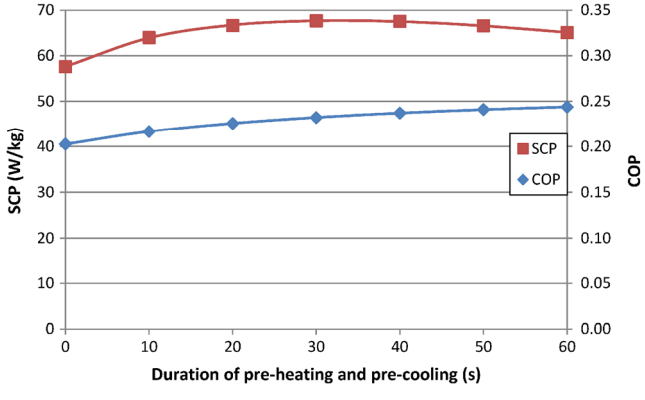

Fig. 13 Effect of duration of pre-heating and pre-cooling in pre-heating and pre-cooling cycle on system performance

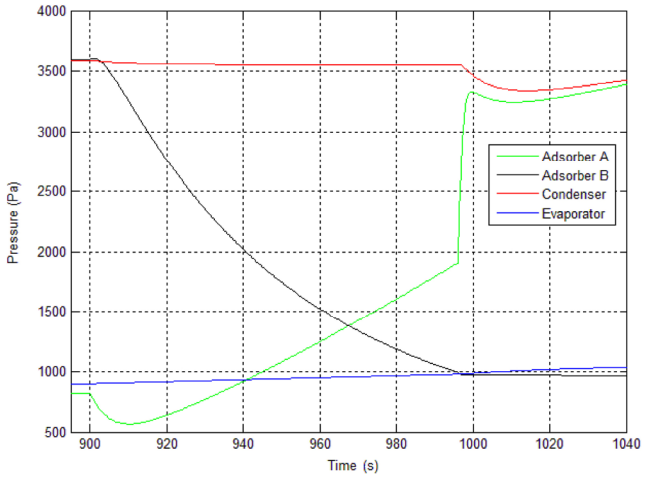

Fig. 14 Pressure profile during the pre-heating and pre-cooling process

There is a slight increase in the evaporator's pressure when the Adsorber B is connected to the evaporator. It was also found that the increase in evaporator temperature during the phase change is about 2.0℃, while that in the basic cycle is about 3.3℃. It should also be pointed out that the duration of the pre-heating process is longer than that of the pre-cooling process based on the results presented in Fig. 14. In the following simulations, the pre-heating and pre-cooling processes have the same duration in order to simplify the procedure.

4.6 Effect of heat and mass recovery cycle

In the previous sections, the best durations for the heat recovery and mass recovery were found to be 30 seconds and 100 seconds, respectively. The optimized durations of heat recovery and mass recovery in the heat and mass recovery cycle, however, may be different from these two values. Thus, a matrix of different durations of heat recovery and mass recovery was tested. In the simulation procedure, both heat and mass recovery processes are conducted for the first portion. After that, the mass recovery process will be stopped while heat recovery will be continued for the remaining duration if the duration of mass recovery process is shorter than that of the heat recovery cycle. For example, the durations of heat recovery and mass recovery are set to be 50 seconds and 20 seconds, respectively. Both heat and mass recovery are conducted for the first 20 seconds. After 20 seconds, mass recovery is stopped and heat recovery continues to be conducted continuously for the remaining 30 seconds. A combined heat and mass recovery cycle was performed by this sequence, and the result is shown in Fig. 15. The SCP is shown in Fig. 15(a), while the COP is shown in Fig. 15(b). From the figure, the best SCP was found

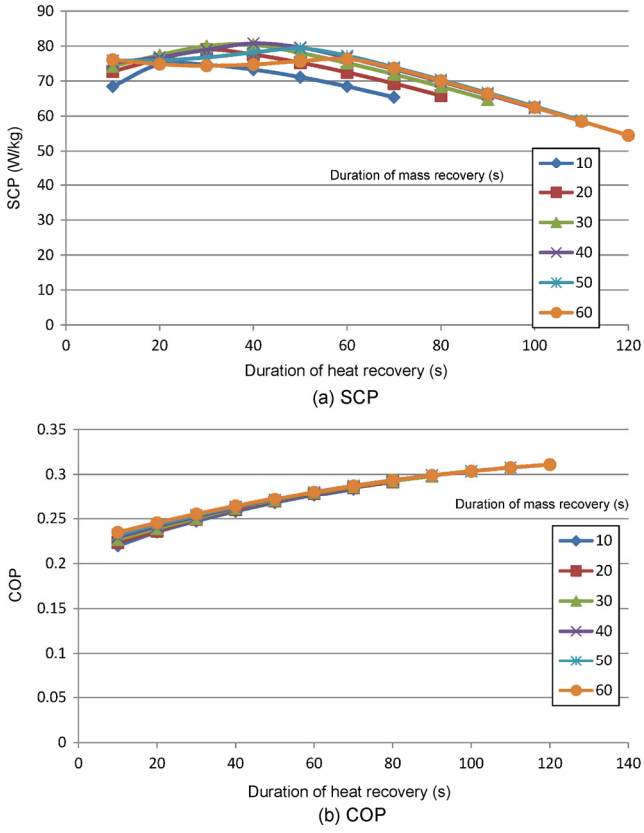

Fig. 15 Effect of duration of heat recovery and mass recovery in heat and mass recovery cycle on system performance

when conducting both the heat and mass recovery processes for 40 seconds. It is interesting to note that the best SCP performance occurred when both heat and mass recovery processes are conducted for 40 seconds, while the optimized duration was 100 seconds for performing the mass recovery process only. This is because heat recovery reduces the temperature difference as well as the pressure difference between the adsorbers. Mass recovery in the heat and mass recovery cycle requires a longer duration than performing only the mass recovery process. The maximum COP and SCP were found to be 0.26 and 80.8 W/kg, respectively. It can also be observed that the lines representing the different duration of mass recovery were very close in Fig. 15(b). This proves that the duration of mass recovery shows a slight influence on the COP, and that it is more dominated by the duration of the heat recovery cycle.

4.7 Effect of heat recovery followed by pre-heating and pre-cooling cycle

In this section, the heat recovery was performed first, followed by a pre-heating and pre-cooling process. From Fig. 16(a), it can be seen that performing the heat recovery showed a negative effect on the SCP in the heat recovery

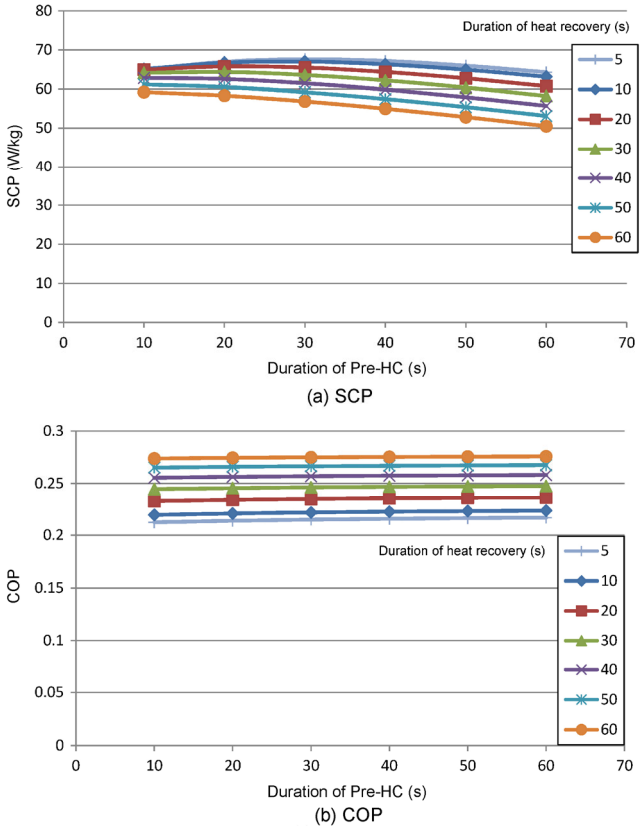

Fig. 16 Effect of duration of HR and Pre-HC in HR followed by Pre-HC cycle on system performance

followed by pre-heating and pre-cooling cycle. The SCP when conducting this cycle was even lower than that of the basic cycle when the total duration of heat recovery and pre-heating and pre-cooling was 90 seconds or longer. The maximum SCP was 67.7 W/kg when the heat recovery and pre-heating and pre-cooling cooling cycle were conducted for 5 seconds and 30 seconds, respectively. The SCP was just slightly lower than that when only performing the pre-heating and pre-cooling process for 30 seconds. Hence, heat recovery followed by a pre-heating and pre-cooling cycle is not recommended if the SCP is the optimization target. The cycle of pre-heating and pre-cooling only should be performed for those adsorption cooling systems which cannot perform the mass recovery cycle. Some additional system components for heat recovery are also not required. This can reduce the cost and simplify the control program of the adsorption cooling systems.

4.8 Effect of mass recovery followed by pre-heating and pre-cooling process

Unlike heat recovery followed by pre-heating and pre-cooling, mass recovery followed by pre-heating and pre-cooling can significantly improve the SCP. The SCP with various durations of mass recovery and pre-heating and pre-cooling cycles is shown in Fig. 17(a). A maximum SCP exists for each of the duration of mass recovery process. Among these, 80 seconds of the mass recovery duration and 20 seconds of the pre-heating and pre-cooling duration had the highest value of SCP, achieving 81.4 W/kg, a 41% improvement compared with that of the basic cycle. The COP was also improved by 15% to 0.23, as shown in Fig. 17(b). It was also found that the COP increases with the duration of the mass recovery process. This agrees with the results of only performing the mass recovery process, in that the COP was improved slightly.

4.9 Effect of heat and mass recovery followed by pre-heating and pre-cooling cycle

It is predicted that for the most optimized system performance, all the processes should be conducted as each process has its individual benefit to the cooling performance of adsorption cooling systems. Based on our results, the ideal duration for performing the heat recovery and mass recovery processes are the same. Based on the results as shown in Fig. 18, the

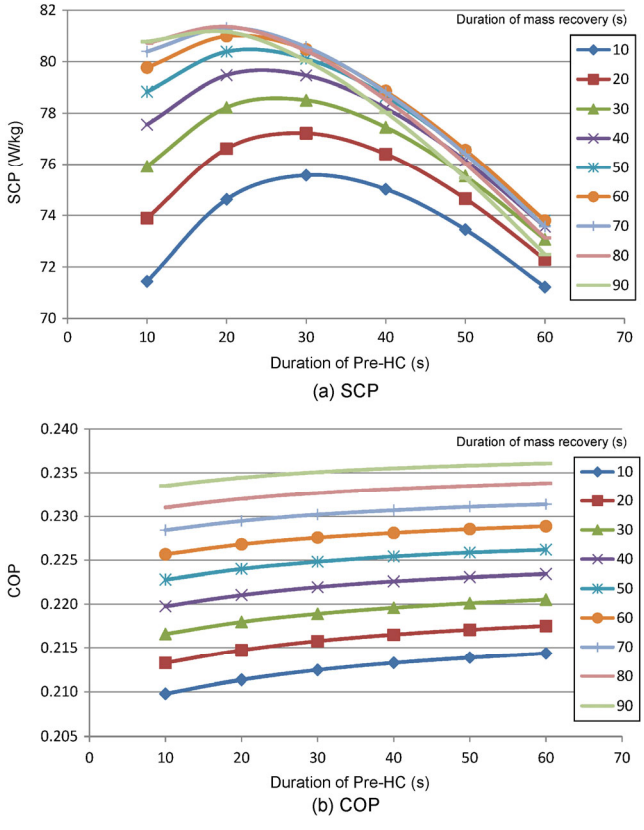

Fig. 17 Effect of duration of MR and Pre-HC in MR followed by Pre-HC cycle on system performance

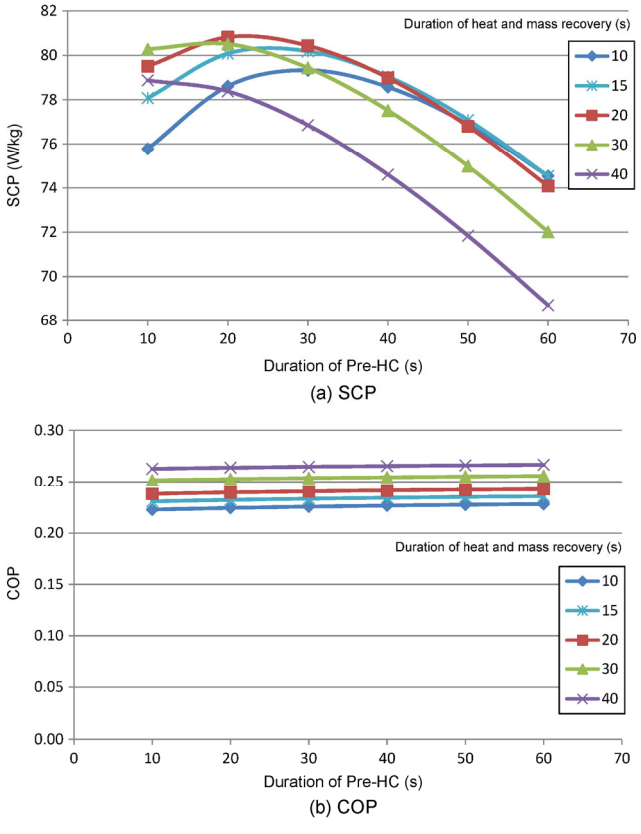

Fig. 18 Effect of duration of HMR and Pre-HC in HMR followed by Pre-HC cycle on system performance

best system performance was obtained at heat and mass recovery for 20 seconds followed by pre-heating and pre-cooling process for 20 seconds. The SCP and COP were calculated at 80.8 W/kg and 0.24 respectively. In comparison with those of the basic cycle, the percentage improvements were 40% and 18%, respectively. Also, the best SCP was slightly lower than that of the mass recovery followed by pre-heating and pre-cooling cycle. This may be due to the fact that the major reason for conducting the heat recovery cycle is to improve the COP, instead of the SCP. In order to perform the heat recovery cycle, an additional water pump, two valves and some pipelines have to be added (Pump 4, V15 and V16 shown in Fig. 1). If the electricity consumption of the system components is included in calculating the COP, the mass recovery followed by pre-heating and pre-cooling cycle would have a much higher COP than that of the heat and mass recovery followed by pre-heating and pre-cooling cycle. Thus, the mass recovery followed by pre-heating and pre-cooling cycle is preferred for most adsorption cooling systems. The cooling performance of the adsorption cooling systems at different operating sequences is summarized in Table 3.

Table 3 Summary of the system performance for different operating sequences

	COP	% increase	SCP (W/kg)	% increase
Basic cycle	0.20	N.A.	57.6	N.A.
HR for 30 s	0.24	20%	66.4	15%
MR for 100 s	0.23	14%	80.8	40%
Pre-HC for 30 s	0.23	15%	67.7	17%
HMR for 40 s	0.26	29%	80.8	40%
HR for 5 s followed by Pre-HC for 30 s	0.21	6%	67.6	17%
MR for 80 s followed by Pre-HC for 20 s	0.23	15%	81.4	41%
HMR for 20 s followed by Pre-HC for 20 s	0.24	18%	80.8	40%

5 Conclusions

In this study, a simulation was conducted to investigate the effect of heat recovery, mass recovery, pre-heating and pre-cooling cycles and their combinations on the system performance of a double-bed adsorption cooling system. The simulation model adopted in this study is more complete than those used in many other studies, due to its consideration of the pressure variations of system components. The water vapor flow between different system components was considered in the simulation such that the mass recovery and pre-heating and pre-cooling processes can be studied. The simulation model was also verified by the experiment results of the double-bed adsorption cooling system prototype. The simulation can closely predict the performance of the real system, showing the high accuracy of the simulation. Based on the simulation results, heat recovery, mass recovery, and pre-heating and pre-cooling cycles show advantages over the basic cycle in the same operating conditions. The following are the conclusions made based on this study:

1) By conducting the heat recovery process for 90 seconds, the COP was significantly increased by 45% to 0.29 compared to that of the basic cycle. On the other hand, heat recovery can also increase the SCP by 15% to 66.4 W/kg with a 30-second duration of the heat recovery process.
2) Mass recovery can significantly increase the SCP. The SCP and COP were increased by 40% and 14% to 80.8 W/kg and 0.23, respectively by conducting the mass recovery process for 100 seconds.
3) The benefit of performing the pre-heating and pre-cooling cycle is smaller than that of the heat recovery and/or mass recovery cycles. The SCP and COP were only increased by 17% and 15% to 67.7 W/kg and 0.23, respectively.
4) For those adsorption cooling systems which cannot carry out the mass recovery process, performing the pre-heating and pre-cooling only cycle is preferred. This means that

it is not necessary to perform the heat recovery cycle if the SCP is the optimization target. Some additional system components can be eliminated if the heat recovery cycle is not performed. Some additional system components for heat recovery are not required. This can reduce the cost and simplify the control program of the adsorption cooling systems.

5) The mass recovery followed by pre-heating and pre-cooling cycle is preferred for most adsorption cooling systems to improve both the COP and SCP. The improvements were 41% for the SCP, increasing to 81.4 W/kg, and 15% for the COP, increasing to 0.23.

Acknowledgements

Funding sources for this research are provided by the Hong Kong Research Grant Council via General Research Fund account 611212 and 16201114 as well as the Science and Technology Program of Guangzhou, China, via Grant No. 2013J4500064.

References

Akahira A, Alam KCA, Hamamoto Y, Akisawa A, Kashiwagi T (2004). Mass recovery adsorption refrigeration cycle-improving cooling capacity. *International Journal of Refrigeration*, 27: 225–234.

Akahira A, Alam KCA, Hamamoto Y, Akisawa A, Kashiwagi T (2005). Experimental investigation of mass recovery adsorption refrigeration cycle. *International Journal of Refrigeration*, 28: 565–572.

Chan KC, Chao CYH, Sze-To GN, Hui KS (2012). Performance predictions for a new zeolite 13X/$CaCl_2$ composite adsorbent for adsorption cooling systems. *International Journal of Heat and Mass Transfer*, 55: 3214–3224.

Chua HT, Ng KC, Malek A, Kashiwagi T, Akisawa A, Saha BB (1999). Modeling the performance of two-bed, sillica gel–water adsorption chillers. *International Journal of Refrigeration*, 22: 194–204.

Chua HT, Ng KC, Wang W, Yap C, Wang XL (2004). Transient modeling of a two-bed silica gel–water adsorption chiller. *International Journal of Heat and Mass Transfer*, 47: 659–669.

Dean JA, Lange NA (1999). Lange's Handbook of Chemistry. New York: McGraw-Hill.

Leong KC, Liu Y (2004). Numerical modeling of combined heat and mass transfer in the adsorbent bed of a zeolite/water cooling system. *Applied Thermal Engineering*, 24: 2359–2374.

Leong KC, Liu Y (2006). System performance of a combined heat and mass recovery adsorption cooling cycle: A parametric study. *International Journal of Heat and Mass Transfer*, 49: 2703–2711.

Liu YL, Wang RZ, Xia ZZ (2005). Experimental study on a continuous adsorption water chiller with novel design. *International Journal of Refrigeration*, 28: 218–230.

Maggio G, Freni A, Restuccia G (2006). A dynamic model of heat and mass transfer in a double-bed adsorption machine with internal heat recovery. *International Journal of Refrigeration*, 29: 589–600.

Munson BR, Young DF, Okiishi TH (2006). Fundamentals of Fluid Mechanics, 5th edn. New York: John Wiley & Sons.

Ng KC, Wang X, Lim YS, Saha BB, Chakarborty A, Koyama S, Akisawac A, Kashiwagi T (2006). Experimental study on performance improvement of a four-bed adsorption chiller by using heat and mass recovery. *International Journal of Heat and Mass Transfer*, 49: 3343–3348.

Pons M (1997). Analysis of the adsorption cycles with thermal regeneration based on the entropic mean temperatures. *Applied Thermal Engineering*, 17: 615–627.

Qu TF, Wang RZ, Wang W (2001). Study on heat and mass recovery in adsorption refrigeration cycles. *Applied Thermal Engineering*, 21: 439–452.

Saha BB, Koyama S, Kashiwagi T, Akisawa A, Ng KC, Chua HT (2003). Waste heat driven dual-mode, multi-stage, multi-bed regenerative adsorption system. *International Journal of Refrigeration*, 26: 749–757.

Sakoda A, Suzuki M (1984). Fundamental study on solar powered adsorption cooling system. *Journal of Chemical Engineering of Japan*, 17: 52–57.

Tso CY, Chao CYH (2012). Activated carbon, silica-gel and calcium chloride composite adsorbents for energy efficient solar adsorption cooling and dehumidification systems. *International Journal of Refrigeration*, 35: 1626–1638.

Tso CY, Chao CYH, Fu SC (2012). Performance analysis of a waste heat driven activated carbon based composite adsorbent–water adsorption chiller using simulation model. *International Journal of Heat and Mass Transfer*, 55: 7596–7610.

Tso CY, Fu SC, Chao CYH (2014). Modeling a solar-powered double bed novel composite adsorbent (silica activated carbon/$CaCl_2$)–water adsorption chiller. *Building Simulation*, 7: 185–196.

Wang DC, Xia ZZ, Wu JY, Wang RZ, Zhai H, Dou WD (2005a). Study of a novel silica gel–water adsorption chiller. Part I. Design and performance prediction. *International Journal of Refrigeration*, 28: 1073–1083.

Wang RZ (2001). Performance improvement of adsorption cooling by heat and mass recovery operation. *International Journal of Refrigeration*, 24: 602–611.

Wang X, Chua HT, Ng KC (2005b). Experimental investigation of silica gel–water adsorption chillers with and without a passive heat recovery scheme. *International Journal of Refrigeration*, 28: 756–765.

Wang X, Ng KC, Chakarborty A, Saha BB (2007). How heat and mass recovery strategies impact the performance of adsorption desalination plant: theory and experiments. *Heat Transfer Engineering*, 28: 147–153.

Zhang LZ, Wang L (1997). Performance estimation of an adsorption cooling system for automobile waste heat recovery. *Applied Thermal Engineering*, 17: 1127–1139.

Zhang LZ (2000). A three-dimensional non-equilibrium model for an intermittent adsorption cooling system. *Solar Energy*, 69: 27–35.